Stretching a Single Diblock Copolymer in a Selective Solvent: Langevin Dynamics Simulations

Scott A. Edwards* and David R. M. Williams

Research School of Physical Sciences, Institute of Advanced Studies, Australian National University, ACT 0200, Australia

Received January 10, 2005; Revised Manuscript Received April 6, 2005

ABSTRACT: Using the Langevin dynamics technique, we have carried out simulations of a single-chain flexible diblock copolymer. The polymer consists of two blocks of equal length, one very poorly solvated and the other close to θ-conditions. We study what happens when such a polymer is stretched, for a range of different stretching speeds, and correlate our observations with features in the plot of force vs extension. We find that at slow speeds this force profile does not increase monotonically, in disagreement with earlier predictions, and that at high speeds there is a strong dependence on which end of the polymer is pulled, as well as a high level of hysteresis.

1. Introduction

Many studies have appeared in recent years on the subject of stretching single molecules. For the most part, these have been inspired by the development of technologies that allow the manipulation of single molecules and studies of their elastic response—in particular, atomic force microscopy (AFM) and optical tweezers. Many such studies have focused on stretching proteins such as titin[1−3] with the aim of deducing clues about the relationship between the structure and function of these complex polymers. However, interpreting the results of such experiments can in general be very difficult owing to the hierarchies of secondary and tertiary structure existing within folded proteins. At the other end of the complexity scale, even the very simple case of a flexible homopolymer in a poor solvent exhibits nontrivial behavior, and new discoveries are still being made about this system.[4−8] An example of relevance to the present paper is the recent discovery (via simulations) of a novel "unraveling" transition[7] in which the collapsed globule spontaneously disintegrates after having a tether pulled from it for some critical distance. This transition was predicted via a simple free energy minimization and demonstrated using Langevin dynamics simulations of a poorly solvated homopolymer.

A diblock copolymer bridges the complexity gap between these two extremes; while still being a much simpler molecule than any protein, it can form multidomain secondary structures in the right solvent conditions. Using the Langevin dynamics technique, we have simulated the stretching of a single diblock copolymer, one block of which is very poorly solvated and the other close to θ-conditions. Previous studies of this class of polymer, notably the HP model of protein folding,[10−13] have focused mainly on random or "evolved" monomer sequences. For simplicity, we study a polymer consisting of only two contiguous blocks of equal length. A theoretical study of this system under quasi-static (equilibrium) pulling has been carried out previously by Lee et al.,[9] at the level of scaling theory. We show that this scaling arguments misses an important aspect of the equilibrium stretching behavior, namely, that the force does not increase monotonically with the extension but rather exhibits a strong dip corresponding to the unraveling transition.[7] We also go beyond equilibrium conditions to study the nonequilibrium effects which become important at high speeds. We find that the stretching behavior under these conditions can be different depending on which end of the chain is pulled and that these differences increase with the stretching speed.

* Corresponding author. E-mail: sae110@rsphysse.anu.edu.au.

2. Model

We use the Langevin dynamics technique to simulate our model polymer. The position of each monomer at a given time step is determined by solving the discretized Langevin equation:

$$r_\alpha(t + \Delta t) = r_\alpha(t) - \frac{1}{\zeta}\frac{\delta V}{\delta \alpha}\Delta t + \eta(t)\sqrt{D} \qquad (1)$$

Here r_α is a Cartesian component of the position vector for the monomer ($\alpha = x, y,$ or z), V is the total potential energy of the monomer, and ζ is the friction coefficent. The term $\eta(t)\sqrt{D}$ accounts for fluctuations due to random collisions with solvent molecules; η is a stochastic variable with mean 0 and variance $2\Delta t$, and $D = kT/\zeta$ is the diffusion constant.

The monomers are treated as spherical beads interacting via a Lennard-Jones (LJ) 6−12 potential:

$$V_{\mathrm{LJ}}(i,j) = 4\epsilon\left[\left(\frac{\sigma}{r(i,j)}\right)^{12} - S\left(\frac{\sigma}{r(i,j)}\right)^{6}\right] \qquad (2)$$

where $r(i,j)$ is the distance separating monomers i and j, and S is a scaling factor used to modify the strength of the attractive interaction depending on monomer type (discussed in more detail below). We set the energy scale of the LJ interaction to be $\epsilon = 3.0kT$. In our simulation we scale all distances by σ, so there is no need to explicitly set its value.

Consecutive beads are connected by springs, which are modeled with the finitely extensible nonlinear

10.1021/ma0500483 CCC: $30.25
Published on Web 11/15/2005

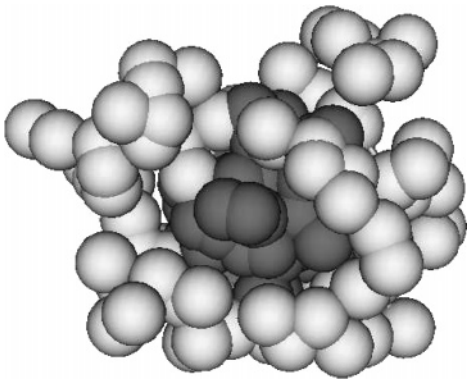

Figure 1. A snapshot of the collapsed equilibrium configuration of the diblock copolymer. The dark beads are type A monomers, and the light beads type B monomers.

elastic (FENE) potential:

$$V_{sp}(i,j) = -\frac{3r_{max}}{a^2}\ln\left(1 - \frac{r(i,j)}{r_{max}}\right) \quad (3)$$

We set the bond length to be $a = 2\sigma$ and the maximum extension to be $r_{max} = 2.1\sigma$. The polymer is fully flexible, meaning there is no energy penalty for bending.

In all simulations discussed in this paper, the polymer has $N = 200$ monomers, split evenly into two blocks—one of type A monomers and the other of type B. There are three possible types of monomer−monomer interaction (AA, BB, and AB), and the strength of the attractive part of the LJ interaction can in general be set differently for each type via the S parameter in eq 2. We were interested in studying a polymer with a specific, simple collapsed state: a hydrophobic core surrounded by a less hydrophobic shell. We modified the S parameter for each type of interaction by trial and error until the desired collapsed configuration was achieved when the polymer was allowed to equilibrate. We chose the AA interaction to be strongly attractive ($S_{AA} = 2$) and the BB interaction to be weakly attractive ($S_{BB} = 0.5$), which corresponds to the type A monomers being in a very poor solvent and the type B monomers being in a slightly poor solvent, close to θ-conditions. There was also a moderate attraction between type A and type B monomers $S_{AB} = 1.5$, but this was low enough compared to the AA interaction that the types were immiscible. In fact, our results are not very sensitive to the choice of S_{AB}—later tests with $S_{AB} = S_{AA}$ show almost identical behavior. The time step was set to be $5 \times 10^{-3}\zeta\sigma^2/kT$. Note that our model uses dimensionless variables, scaled by kT where appropriate, so there is no need to explicitly set the temperature T.

In each simulation run, the polymer was first allowed to equilibrate for 5×10^5 time steps, during which it would quickly adopt the ground-state conformation shown in Figure 1: a central globule of type A monomers surrounded by a loose shell of type B monomers. Note that this configuration relies on our particular choice of monomer sequence; in general, different sequences of A and B monomers will have different ground states and exhibit richer behavior on stretching. After equilibration, the polymer was stretched by fixing the position of the bead at one end of the chain and gradually stepping the z coordinate of the bead at the other end, leaving it free to move in the x and y directions. At a given extension, the pulling direction was reversed and the polymer unstretched. Throughout this cycle, the net force in the z direction acting on the pulled bead was recorded, after averaging over every 5000 time steps (2000 time steps for the fastest pulling speed). It is important to note that *extension* is the independent variable in this stretching process, in contrast with other studies of stretching HP protein models in which *force* is the independent variable.[10,11]

We simulated stretching at pulling speeds ranging from $0.0001\sigma/\Delta t$ to $0.0015\sigma/\Delta t$. There are two ways the polymer can be stretched in our model: either the type B end of the chain is fixed while the type A end is pulled, or vice versa. In what follows, we refer to pulling the type A end as "method A" and pulling the type B end as "method B" . We simulated both methods at each pulling speed for comparison. Every simulation was repeated five times—in every case, there were no significant differences between the results of repeats.

3. Results

At the lowest pulling speed ($0.0001\sigma/\Delta t$), there was little difference between the force−extension curves generated by the two methods. In both cases, the stretching process proceeds in a number of distinct stages, the transitions between which are clearly identified with features in the force−extension plots (Figures 2 and 3). First, the type B "shell" is unpeeled. During this stage the force stays roughly constant on average. Second, the unpeeled type B block is stretched out, causing the force to increase linearly. Once the force reached a critical value, the type A globule undergoes the "tadpole" transition first identified by Halperin and Zhulina,[4] in which a tether is pulled from the globule. In this third stage (referred to below as the "plateau" stage), the force drops slowly as the size of the globule decreases. Then another transition, the unraveling transition,[7] occurs—the globule suddenly disintegrates, and the force consequently drops suddenly as extra slack is introduced to the chain. In the final stage of stretching, the entire chain is extended and the force once again increases linearly. The unstretching process is essentially the stretching process in reverse, although there is some hysteresis in that the type A globule reforms at a lower extension than the one at which it initially disintegrates during stretching. The plateau phase is consequently shorter, as there is more slack in the chain when the globule re-forms, and it is quickly able to "eat" the rest of the type A block.

The stages described above correspond for the most part with those predicted by Lee et al.[9] using scaling arguments, but there are some notable differences. One of these is our lack of an initial stretching phase before the peeling of the type B block from the surface of the globule. This is likely just a reflection of the relatively low strength of the AB attraction in our simulations, coupled with the fact that only a small fraction of the type B monomers are adsorbed at the globule surface at any given time. Thus, only a small force is required to peel the block from the surface. A much more fundamental difference, however, is the sudden dip in the force profile corresponding to the unraveling transition. The resulting peak is the most distinctive feature in the force profile but would be unexpected if the unraveling transition was not taken into account.

At this low pulling velocity there are two notable differences between the force−extension plots for each stretching method. First, there is much more noise

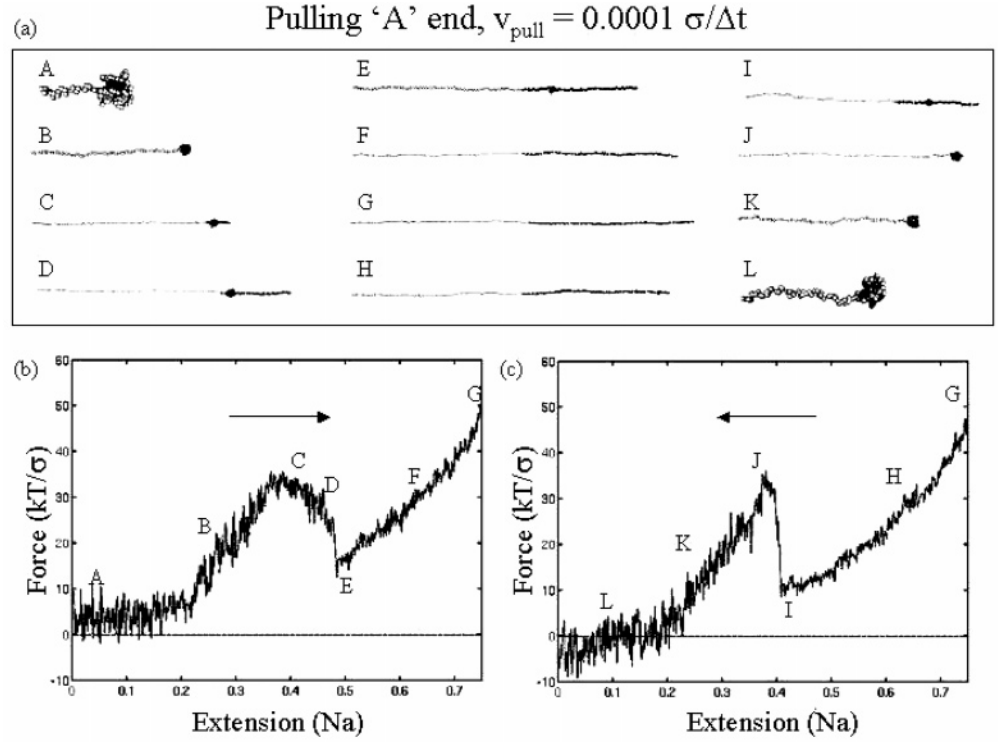

Figure 2. (a) Snapshots of the diblock copolymer during the simulated stretching−unstretching process. The stretching velocity is $v_{pull} = 0.0001\sigma/\Delta t$, and pulling is from the type A end of the polymer. The dark beads are type A, and the light beads are type B. (b) Force plotted as a function of extension for the stretching phase of the cycle. Extension is given in units of the total extended length of the polymer, Na. The letters correspond to the snapshots in part (a). (c) As for part (b), but for the unstretching phase of the cycle.

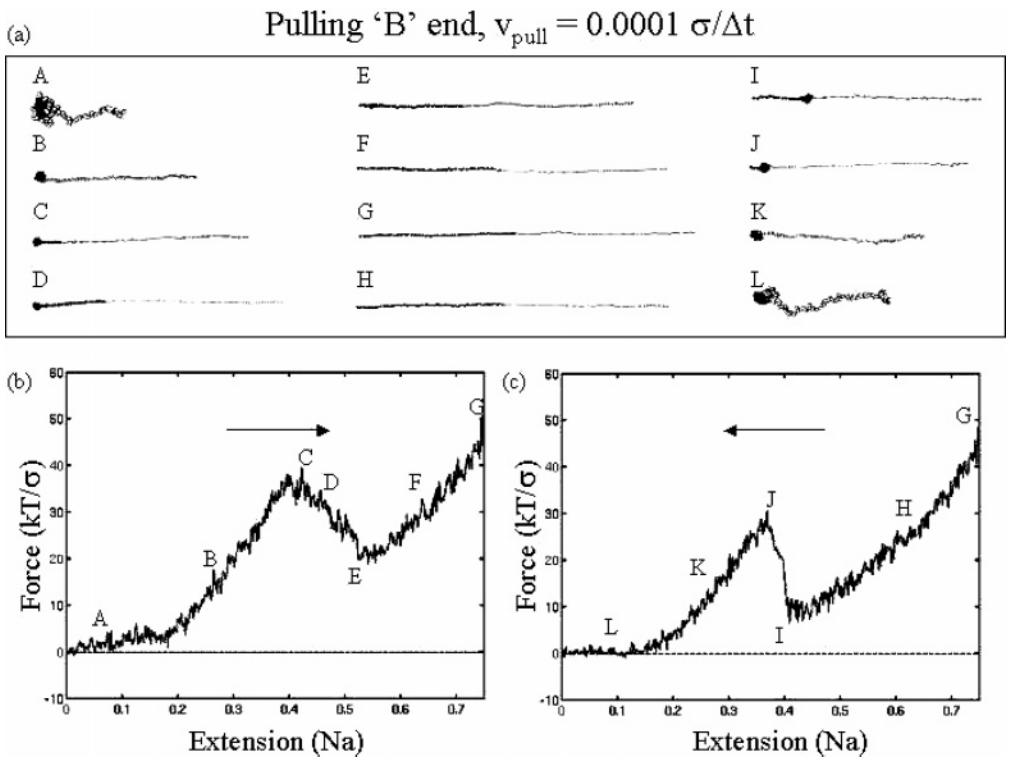

Figure 3. As for Figure 2, but pulling from the type B end of the polymer.

evident at the beginning and end of the stretching cycle for method A, compared with method B. This is because in the former case the pulled bead is inside the globule of type A beads during these stages of the cycle and is thus subjected to a rapidly varying potential energy profile. In contrast, the pulled bead in method B is only influenced directly by its neighboring bead. The second notable difference is that the force goes negative at the end of the unstretching process for method A, but not for method B. Again, this is due to the globule, which in method A gets dragged along with the pulled bead. The drag force due to the globule acts in the opposite direction to the pulling, which amounts to a negative force (in the positive z direction) during unstretching.

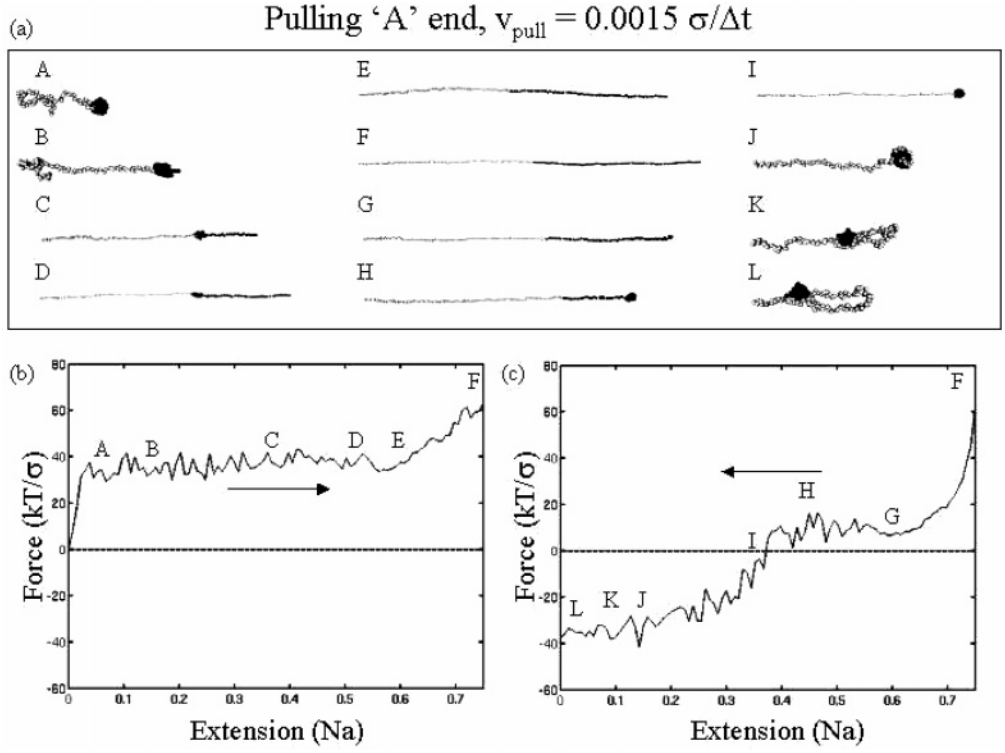

Figure 4. As for Figure 2, but with a pulling velocity of $v_{pull} = 0.0015\sigma/\Delta t$.

In method B the globule stays stationary near the fixed type A end of the chain and does not contribute to the drag.

At higher pulling speeds, the differences between the two stretching methods are much more striking, as are the differences between the stretching and unstretching halves of an individual cycle. This is most clearly evident in the results for the highest stretching speed we simulated, $0.0015\sigma/\Delta t$. For method A (Figure 4), the force profile immediately rises to a plateau and stays that way for most of the stretching process. From examining the snapshots of the polymer conformation, we see that this is because the "tadpole" transition occurs almost immediately after stretching begins, even while the type B block is still partially coiled. There is no drop in force when the globule disintegrates, in contrast with the slow stretching case; the slack generated by the globule disintegrating is taken up immediately. Only when the entire chain becomes stretched does the force deviate from the plateau and begin rising again. During the unstretching half of the cycle, the force becomes strongly negative once the globule has reformed, in strong contrast to the behavior seen during the first half of the cycle. This is again due to the drag developed in having to pull the globule along with the end bead, and clearly this drag dominates much more here than in the slow stretching case. Also, a hairpin bend occurs in the type A block toward the end of the unstretching process. This is a reflection of the strongly nonequilibrium nature of such fast stretching—the chain has no time to relax as the end bead is rushed to and fro, in contrast with the slow stretching case discussed above.

The fast-stretching results for method B are given in Figure 5. Instead of the "tadpole" transition happening straight away, as was seen for method A, it actually occurs slightly later in the stretching process than it does for slow stretching. This is reflected in the force–extension plot rising monotonically for the first two-thirds of the process; only in the final third does the plateau corresponding to the pull-out of a tether from the globule occur. This plateau is at a much higher force than was observed for slow stretching, or for method A at any stretching speed, a point that will be discussed further below. For the unstretching process, the force profile is almost featureless, dropping smoothly and monotonically (apart from random fluctuations) for the entire process. This is due to the formation of a hairpin bend in the type B block, which occurs before the reformation of the globule and other events that would otherwise show up as features in the force profile. Because of the hairpin, however, information about these events does not reach the end bead, the force on which is determined from then on only by the drag of the rest of the chain. This drag is naturally much less than that of the globule in method A.

One intriguing aspect of the force–extension plots for method B, touched on earlier, is that the height of the force plateau corresponding to the tadpole transition (the pull-out of a tether from the globule) depends on the pulling velocity. This trend is shown explicitly in Figure 6, which plots the height of the force plateau vs pulling speed. We saw no such trend for method A—the tadpole transition always occurred at a force of $(35 \pm 5)kT/\sigma$ regardless of the pulling speed. The trend plotted in Figure 6 tends to this same value in the limit of zero pulling velocity; it corresponds closely to the maximum attractive value of the LJ force between two type A beads, which is $32.3kT/\sigma$ (corresponding to a bead separation of about 1.1σ). The presence of this trend in the method B results seems to be due to the drag of the type B block itself as its free end is pulled away from the globule. At slow speeds, this drag is negligible, as is reflected in the initial flatness of the force profile in Figure 3b; at this speed, the force only starts to go up once the type B block is extended and the begins to pull

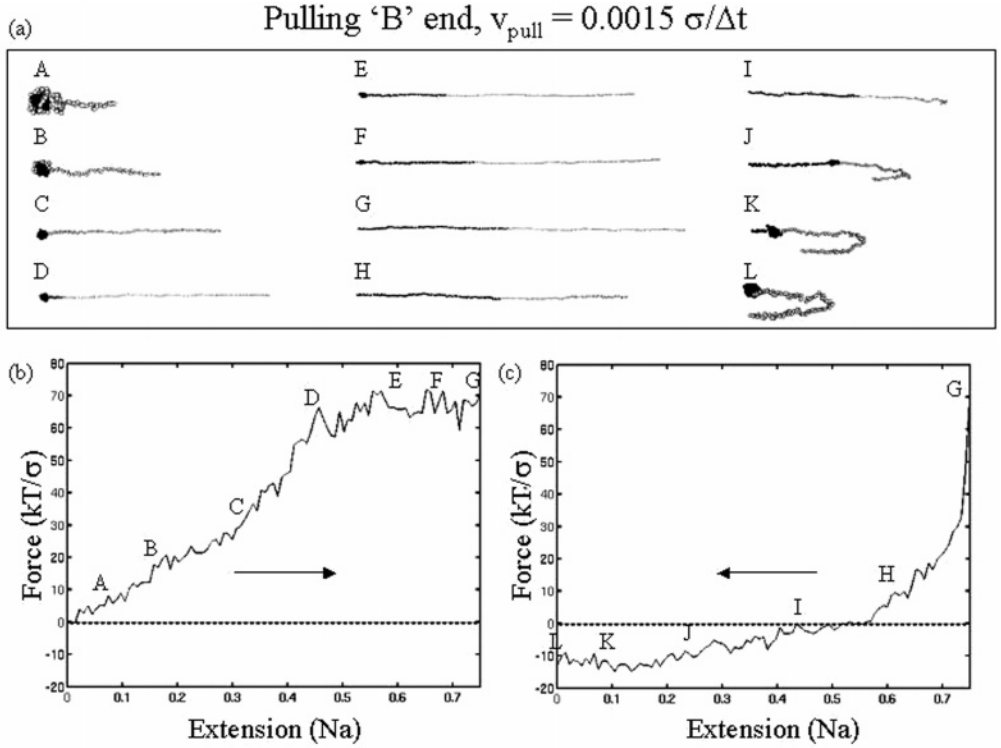

Figure 5. As for Figure 2, but with a pulling velocity of $v_{pull} = 0.0015\sigma/\Delta t$ and pulling from the type B end of the polymer.

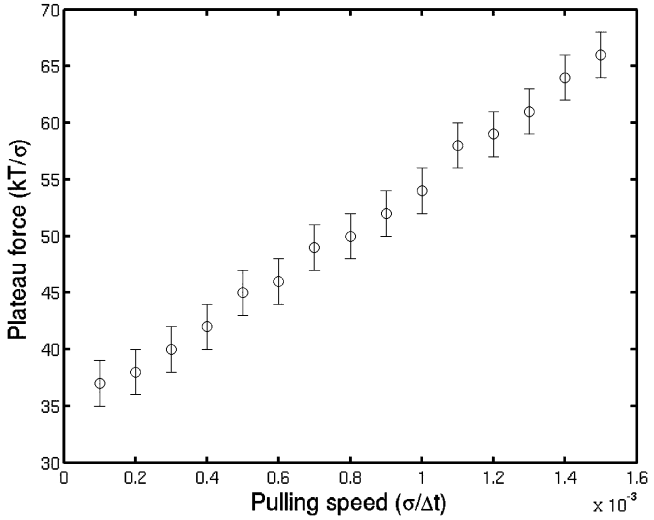

Figure 6. Plot of the observed "plateau" force (the force at which the tadpole transition occurs during stretching) vs pulling speed for stretching method B (pulling the type B end of the polymer).

on the type A globule. As the stretching speed is increased, however, the type B block has more and more difficulty keeping up with the pulled end. The resulting drag generates a significant restoring force on the pulled bead well before the type B block is extended, as is evident in Figure 5b. When the tadpole transition occurs, the force on the pulled bead is due not only to deforming the globule but also to this drag force, and thus the height of the force plateau increases as the stretching speed (and therefore the drag on the type B block) increases.

We identify two primary shortcomings with our simulations. The first relates to the time scale. The slowest pulling speed that we can conveniently simulate, $0.0001\sigma/\Delta t$, corresponds to a real velocity on the order of 1 mm/s if typical values of σ, ζ, and kT for a protein in water are chosen ($\sigma \simeq 1$ nm, $\zeta \simeq 2 \times 10^{-11}$ kg s^{-1}, and $kT = 4.2 \times 10^{-21}$ J). In comparison, typical AFM stretching experiments stretch at rates on the order of 1 μm/s, 3 orders of magnitude slower. Thus, the results seen in our fastest-stretching-speed simulations are probably not accessible to current experimental methods. However, we expect that our slowest stretching speed is still close to quasi-static conditions and that results would not be qualitatively different for much slower speeds. Evidence that this is so comes from the height of the force plateau, discussed in the previous paragraph. At our slowest stretching speed, $v_{pull} = 0.0001\sigma/\Delta t$, the plateau force is about the same (around $35kT/\sigma$) for both stretching methods, suggesting that in method B the type B block has sufficient time to relax as it is stretched. We ran a single simulation run at the much slower speed of $v_{pull} = 1 \times 10^{-5}\sigma/\Delta t$ and found that the same was true in this case as well. In fact, there were no other significant differences between the stretching behavior at this very slow speed and at $v_{pull} = 0.0001\sigma/\Delta t$, which suggests that at this speed and below nonequilibrium effects are negligible and stretching behavior converges to that expected for quasi-static stretching. We stress that the dip in the force profile due to the unraveling transition has been predicted from purely equilibrium considerations[7] and is not an artifact of high stretching speeds.

The second shortcoming of our simulations is that hydrodynamic screening is not included in our model. This means that the drag generated by the collapsed type A globule in our simulations is significantly higher than it should be. This should not affect our method B results, since the globule is always stationary, but it does mean that our method A results would probably require faster pulling speeds to reproduce if screening was taken into account.

4. Summary

We have simulated the stretching of a diblock copolymer, with one block very poorly solvated and the other close to θ-conditions. At slow pulling speeds we have shown that for the most part stretching proceeds in the distinct stages identified by Lee et al., regardless of which end of the chain is pulled. However, in disagreement with their prediction of a monotonically increasing force with extension, we find that the occurrence of the unraveling transition at a critical extension leads to a sudden and significant drop in the restoring force. Thus, the force profile has a prominent peak at intermediate extension. At very fast pulling speeds, the combined effects of drag and nonequilibrium conditions lead to pronounced differences in the stretching behavior depending on which end of the chain is pulled. In particular, when pulling from the uncollapsed (type B) end of the chain we find that the force at which the Halperin−Zhulina "tadpole" transition occurs increases with pulling speed, while no such trend is evident when pulling from the collapsed (type A) end. There is also strong hysteresis with respect to stretching and unstretching at high speeds.

In general, our results highlight the difficulties inherent in predicting and interpreting the elastic response of even such a simple system as a diblock copolymer—let alone a highly structured protein molecule. Although there have been spectacular advances in this field over the past several years with regards to experiments, progress will rely just as much on theory and modeling to flesh out our understanding of the range of things that can happen when a molecule is stretched and thereby provide a firmer foundation for extracting what does happen in a given specific case from experimental results.

References and Notes

(1) Rief, M.; Gautel, M.; Oesterhelt, F.; Fernandez, J. M.; Gaub, H. E. *Science* **1997**, *276*, 1109.
(2) Kellermayer, M. S. Z.; Smith, S. B.; Granzier, H. L.; Bustamante, C. *Science* **1997**, *276*, 1112.
(3) Tskhovrebova, L.; Trinick, J.; Sleep, J. A.; Simmons, R. M. *Nature (London)* **1997**, *387*, 308.
(4) Halperin, A.; Zhulina, E. B. *Europhys. Lett.* **1991**, *15*, 417.
(5) Haupt, B. J.; Senden, T. J.; Sevick, E. M. *Langmuir* **2002**, *18*, 2174.
(6) Marenduzzo, D.; Maritan, A.; Rosa, A.; Seno, F. *Phys. Rev. Lett.* **2003**, *90*, 088301.
(7) Cooke, I. R.; Williams, D. R. M. *Europhys. Lett.* **2003**, *64*, 267.
(8) Cieplak, M.; Hoang, T. X.; Robbins, M. O. *Phys. Rev. E* **2004**, *70*, 011917.
(9) Lee, N. K.; Johner, A.; Vilgis, T. A. *Macromolecules* **2002**, *35*, 6043.
(10) Lee, N. K.; Vilgis, T. A. *Eur. Phys. J. B* **2002**, *28*, 451.
(11) Geissler, P. L.; Shakhnovich, E. I. *Macromolecules* **2002**, *35*, 4429.
(12) Lau, K. F.; Dill, K. A. *Macromolecules* **1989**, *22*, 3986.
(13) Ramanathan, S.; Shakhnovich, E. *Phys. Rev. E* **1994**, *50*, 1303.

MA0500483